June 23, 2000 LAUR 00-2523

Resumming the large-N approximation for time evolving quantum systems

Bogdan Mihaila,[a,b] Fred Cooper,[c] and John F. Dawson,[a]

(a) Department of Physics,
University of New Hampshire, Durham, NH 03824

(b) Chemistry and Physics Department,
Coastal Carolina University, Conway, SC 29526

(c) Theoretical Division,
Los Alamos National Laboratory, Los Alamos, NM 87545

bogdan.mihaila@unh.edu
cooper@schwinger.lanl.gov
john.dawson@unh.edu

Abstract

In this paper we discuss two methods of resumming the leading and next to leading order in $1/N$ diagrams for the x^4 $O(N)$ model, which seem to preserve both boundedness and positivity for expectation values of operators at all times. These approximations can be understood either in terms of a truncation to the infinitely coupled Schwinger-Dyson hierarchy of equations, or by choosing a particular two-particle irreducible vacuum energy graph in the effective action. The key to these approximations is to treat both the x propagator and the x^2 propagator on similar footing. The bare vertex approximation (BVA) is obtained by replacing the exact vertex function by the bare one in the exact Schwinger-Dyson equations for the one and two point functions. The second approximation, which we call the dynamic Debye screening approximation (DDSA), makes the further approximation of replacing the exact x^2 propagator by its value at leading order in the $1/N$ expansion. We also show how to obtain these results using the effective action of the Cornwall-Jackiw-Tomboulis (CJT) formalism. These two approximations are compared with exact numerical simulations for the quantum roll problem. Both of them cure the defects of the next to the leading order in $1/N$ approximation in that $\langle x^2(t)\rangle$ remains bounded and positive definite at all times. The BVA approximation captures the physics at large and modest N better than the DDSA approximation. It yields accurate results for $\langle x^2(t)\rangle$ at late times in the strong coupling regime when $N \geq 10$.

1 Introduction

The need to understand quantum systems in real time in a quantum field theoretic setting arose from attempts to understand various early universe scenarios. These scenarios are based on the evolution of scalar fields either through their role as inflaton fields or as topological defect forming fields. One would like to understand the quantum evolution of these fields rather than rely on unjustified treatments based on studying their classical evolution. The study of the "slow rollover" transition in an upside down harmonic approximation by Guth and Pi[1] was the first attempt to understand whether classical approximations could be justified. However, one really needed to go beyond the harmonic approximation to address the nonlinear aspects of double well potentials. These non-linear aspects effect production of topological defects as well as the nature of the oscillation at the bottom of the well which causes reheating.

Our goal is to be able to describe the nonlinear aspects of double well physics accurately quantum mechanically. Although in one-dimensional quantum mechanics, one can rely on a numerical solution of the Schrödinger equation to understand this problem, in field theory contexts the numerical solution of the functional Schrödinger equation is presently beyond the reach of the largest computers. Various approximation schemes have been suggested based either upon making a variational approximation to the functional Schrödinger equation, or using the closed-time-path formalism coupled with a $1/N$ expansion to calculate the time evolution of the Green's functions in the Heisenberg picture. The variational approach leads to a Hamiltonian dynamical system for the variational parameters with positive definite probabilities. Thus energy conservation and positivity of certain expectation values are automatically guaranteed. However, even for the simple problem of the quantum roll, the Gaussian, or time dependent Hartree approximation, studied by Cooper, Pi and Stancioff[2], and improvements which are based on trial wave functions of the form of a polynomial times a Gaussian[3], are only accurate for relatively short time periods (one or a few oscillations) when compared to the exact numerical solution of the Schrödinger equation.

If instead of the wave functional, one instead considers the infinitely coupled dynamics of the Green's functions describing the evolution, one soon realizes that one is faced with exactly the same issues that many-body theorists and plasma physicists faced in the 1960's. In both quantum and classical many-body systems, the dynamical equations are an infinite hierarchy of coupled equations which relate given ensemble averages, whether classical or quantum, to successively more complicated ones. To make the solution of this hierarchy possible, some truncation scheme is necessary. Most naive truncation schemes which, for example, just truncate the hierarchy of coupled correlators at a particular order, do not preserve various physical properties required of the system — such as positivity of the spectral components of the Green's function and conservation of probability. A corrollary of this is that in most perturbation schemes, secularity arises quickly with each term in the perturbation series, growing with higher powers of the time t. In his seminal paper of 1961, Robert Kraichnan[4] discussed in detail the key issues and obtained a partial solution to the problem by demanding that the approximations one should use should correspond to some physically realizable

dynamical system. This would guarantee positivity and secularity would be avoided. He also discussed scenarios where particular classes of graphs, which contained the relevant dynamics, are summed and he suggested some physically motivated approximations which did not suffer from any diseases. In field theory one rarely has the parameter control to make such guesses, however some progress in QCD has been made by summing hard thermal loops[5], which already tells us some of the graphs that we want to include. In plasma physics, one wants to make sure that the approximation to the dynamics is robust enough so that the photon propagator includes polarization effects, which give Debye screening. This is related to the hard thermal loop summation in QCD.

In quantum field theory, the approximation that has been used up until now to do time evolution problems has been the leading-order in large-N approximation, or the related Hartree approximation[6, 7]. This is a truncation of the hierarchy at the one and two-point function level. This truncation *is* physical in that one can derive it from a time dependent variational principle, leading to a Hamiltonian evolution for the variational parameters which are the one- and two-point functions themselves. The problem with these mean-field approximations is that they do not include the hard scattering which lead to equilibrium, so that very important questions are not addressable. Naive use of the expansion in $1/N$ for an anharmonic oscillator[8] leads to exactly the problems found by Kraichnan in his discussion of the random oscillator in perturbation theory. After a few oscillations, quantities such as $\langle x^2(t)\rangle$ blow up when we include the $1/N$ correction to the leading order in large-N result. To calculate the conductivity of a non-relativistic plasma, it is known what graphs are necessary to sum in order to get agreement with experimental results[9, 10]. Based on this knowledge and the work of Kraichnan, we have studied two different truncations of the exact Schwinger-Dyson equation and applied them to the problem of the quantum roll — the long time behavior of N coupled anharmonic oscillators with "radial" symmetry in an N-dimensional space. This particular problem has been studied by us previously[8] in the large-N approximation and is interesting because exact numerical solutions can be found for arbitrary N.

In this paper, we present numerical solutions for the quantum roll problem for the $O(N)$ model, and compare them to two different approximations to the Schwinger-Dyson equations, which sum infinite numbers of leading order and next to leading order in $1/N$ graphs. The first approximation, which we call the bare vertex approximation (BVA), uses the full Green's function for x as well as the full Green's function for x^2 in a 2-PI Hartree graph contribution to the effective action. This is equivalent to setting the vertex function to unity in the Schwinger-Dyson equations for the one- and two-point functions with external sources. The second approximation, which we call the dynamic Debye screening approximation (DDSA), makes the further assumption that the full x^2 propagator can be replaced by the lowest order in $1/N$ composite field propagator in all the integral equations. Both these approximations are free from the difficulties found in the perturbative $1/N$ expansion, which we display for comparison. We find that the BVA is quite accurate at late times even for modest values of $N \geq 10$.

2 The $O(N)$ model

The classical Lagrangian for the $O(N)$ model of N non-linear oscillators is given by:

$$L(x,\dot{x}) = \frac{1}{2}\sum_{i=1}^{N}\dot{x}_i^2 - \frac{g}{8N}\left(\sum_{i=1}^{N}x_i^2 - r_0^2\right)^2 . \tag{1}$$

The Schrödinger equation for this problem is given by:

$$\left\{-\frac{1}{2}\sum_{i=1}^{N}\frac{\partial^2}{\partial x_i^2} + V(r)\right\}\psi(x,t) = i\,\frac{\partial\psi(x,t)}{\partial t}\,, \tag{2}$$

where $V(r)$ is a potential of the form

$$V(r) = \frac{g}{8N}\,\left(r^2 - r_0^2\right)^2\,, \qquad r^2 = \sum_{i=1}^{N}x_i^2\,. \tag{3}$$

For the quantum roll problem there is spherical symmetry and we can assume a solution of the form

$$\psi(r,t) = \phi(r,t)/r^{(N-1)/2} \tag{4}$$

In which case the time dependent Schrödinger equation for $\phi(r,t)$ reduces to[11]:

$$\left\{-\frac{1}{2}\frac{\partial^2}{\partial r^2} + U(r)\right\}\phi(r,t) = i\,\partial\phi(r,t)\partial t\,, \tag{5}$$

with an effective one dimensional potential $U(r)$ given by

$$U(r) = \frac{(N-1)(N-3)}{8\,r^2} + \frac{g}{8N}\,\left(r^2 - r_0^2\right)^2\,. \tag{6}$$

It is this equation that we will solve numerically to obtain exact numerical solutions as a function of N. Returning to the Lagrangian formulation, it is useful for the purposes of obtaining a large-N expansion to introduce scaled variables:

$$x_i \to \sqrt{N}x_i\,, \qquad r_0 \to \sqrt{N}r_0\,. \tag{7}$$

Then the Lagrangian scales by a factor of N:

$$L/N = L_N(x,\dot{x}) = \frac{1}{2}\sum_{i=1}^{N}\dot{x}_i^2 - \frac{g}{8}\left(\sum_{i=1}^{N}x_i^2 - r_0^2\right)^2 . \tag{8}$$

We use scaled variables in this paper. Next we introduce a composite coordinate χ by adding to (8) a term:

$$\frac{1}{2g}\Big(\chi - \frac{g}{2}\Big(\sum_{i=1}^{N} x_i^2 - r_0^2\Big)\Big)^2 . \tag{9}$$

The Lagrangian (8) then becomes:

$$L_N(x,\chi;\dot{x},\dot{\chi}) = \frac{1}{2}\sum_{i=1}^{N}\big(\dot{x}_i^2 - \chi\, x_i^2\big) + \frac{r_0^2\,\chi}{2} + \frac{\chi^2}{2g} . \tag{10}$$

It is now useful to extend our notation to include all independent coordinates in one vector. We define:

$$\begin{aligned} x_\alpha(t) &= [\chi(t), x_1(t), x_2(t), \ldots, x_N(t)] , \\ j_\alpha(t) &= [\tilde{J}(t), j_1(t), j_2(t), \ldots, j_N(t)] . \end{aligned} \tag{11}$$

for $\alpha = 0, 1, \ldots, N$, and where $\tilde{J}(t) = J(t) - r_0^2/2$. Absorbing the factor $r_0^2/2$ into the current means that $\tilde{J}(t)$ is not zero when $J(t)$ is set to zero. Greek indices run from 0 to N, whereas Latin indices go from 1 to N. Using this extended notation, the generating functional $Z[j]$ and connected generator $W[j]$ is given by the path integral:

$$Z[j] = e^{i\,NW[j]} = \prod_{\alpha=0}^{N}\int \mathrm{d}x_\alpha\, \exp\Big\{i\,NS_N[x;j]\Big\} \tag{12}$$

where the action $S_N[x;j]$ is given by:

$$S_N[x;j] = -\frac{1}{2}\sum_{\alpha,\beta}\int_{\mathcal{C}}\mathrm{d}t\int_{\mathcal{C}}\mathrm{d}t'\, x_\alpha(t)\,\Delta^{-1}_{\alpha,\beta}[x](t,t')\,x_\beta(t') + \sum_{\alpha}\int_{\mathcal{C}}\mathrm{d}t\, x_\alpha(t)\, j_\alpha(t) , \tag{13}$$

and where $\Delta^{-1}_{\alpha,\beta}[x](t,t')$ is given by:

$$\Delta^{-1}_{\alpha,\beta}[x](t,t') = \begin{pmatrix} D^{-1}(t,t') & 0 \\ 0 & G^{-1}_{ij}[\chi](t,t') \end{pmatrix} , \tag{14}$$

with

$$D^{-1}(t,t') = -\frac{1}{g}\,\delta_{\mathcal{C}}(t,t') , \tag{15}$$

$$G^{-1}_{ij}[\chi](t,t') = \left\{\frac{\mathrm{d}^2}{\mathrm{d}t^2} + \chi(t)\right\}\delta_{ij}\delta_{\mathcal{C}}(t,t') . \tag{16}$$

In what follows it will be useful to introduce another matrix inverse Green's function $G^{-1}_{\alpha\beta}[x](t,t')$ as follows:

$$G^{-1}_{\alpha,\beta}[x](t,t') = -\frac{\delta^2 S_N[x;j]}{\delta x_\alpha(t)\,\delta x_\beta(t')} = \begin{pmatrix} D^{-1}(t,t') & \bar{K}^{-1}_j(t,t') \\ K^{-1}_i(t,t') & G^{-1}_{i,j}(t,t') \end{pmatrix} , \tag{17}$$

with $D^{-1}(t,t')$ and $G^{-1}_{i,j}(t,t')$ given by (15) and (16) respectively, and

$$K^{-1}_i[x](t,t') = \bar{K}^{-1}_i[x](t,t') = x_i(t)\,\delta_{\mathcal{C}}(t,t') . \tag{18}$$

3 The Schwinger-Dyson equations

The Schwinger-Dyson equations are generated by functional differentiation of the generating function of the theory. They produce an infinitely coupled hierachy of coupled equations. For an initial value problem, the time ordering is the closed time path of the Schwinger-Keldysh-Bakshi-Mahanthappa formalism[12] that we used in our discussion of the $1/N$ expansion for this problem[6]. One way to generate the equations is to consider the identity[13]:

$$\prod_\beta \int \mathrm{d}x_\beta \, \frac{\delta}{\delta x_\alpha(t)} \, e^{iN\,S_N[x;j]} = 0 . \tag{19}$$

This gives expectation values of the Heisenberg equations of motion:

$$\begin{aligned} -\frac{1}{g}\,\chi(t) + \frac{1}{2}\left\{ \sum_i \left[x_i^2(t) + \frac{1}{N}\mathcal{G}_{ii}(t,t)/i \right] - r_0^2 \right\} &= J(t) , \\ \left\{ \frac{\mathrm{d}^2}{\mathrm{d}t^2} + \chi(t) \right\} x_i(t) + \frac{1}{N}\mathcal{K}_i(t,t)/i &= j_i(t) . \end{aligned} \tag{20}$$

Green's functions $\mathcal{G}_{\alpha,\beta}[j](t,t')$ are defined by:

$$\mathcal{G}_{\alpha,\beta}[j](t,t') = \frac{\delta x_\alpha(t)}{\delta j_\beta(t')} = \frac{\delta^2 W[j]}{\delta j_\alpha(t)\,\delta j_\beta(t')} = \begin{pmatrix} \mathcal{D}(t,t') & \mathcal{K}_j(t,t') \\ \bar{\mathcal{K}}_i(t,t') & \mathcal{G}_{i,j}(t,t') \end{pmatrix} , \tag{21}$$

where explicitly

$$\begin{aligned} \mathcal{D}(t,t') &= \frac{\delta^2 W[J,j]}{\delta J(t)\,\delta J(t')} \qquad & \mathcal{K}_i(t,t') &= \frac{\delta^2 W[J,j]}{\delta J(t)\,\delta j_i(t')} \\ \bar{\mathcal{K}}_i(t,t') &= \frac{\delta^2 W[J,j]}{\delta j_i(t)\,\delta J(t')} \qquad & \mathcal{G}_{i,j}(t,t') &= \frac{\delta^2 W[J,j]}{\delta j_i(t)\,\delta j_j(t')} \end{aligned}$$

The integrability conditions are $\bar{\mathcal{K}}_i(t,t') = \mathcal{K}_i(t',t)$. The Schwinger-Dyson equations are usually given in terms of the coordinate variables $x_\alpha(t)$, rather than the currents. This

change of variables is accomplished by means of a Legendre transformation to the 1-PI effective action $\Gamma[x]$,

$$\Gamma[x] = W[j] - \int_{\mathcal{C}} \mathrm{d}t \, \sum_{\alpha} \{x_\alpha(t) j_\alpha(t)\} \, . \tag{22}$$

So since $j_\alpha(t) = -\delta\Gamma[x]/\delta x_\alpha(t)$, the equations of motion (20) give values for derivatives of $\Gamma[x]$:

$$-\frac{\delta\Gamma[x]}{\delta\chi(t)} = -\frac{1}{g}\,\chi(t) + \frac{1}{2}\left\{\sum_i \left[x_i^2(t) + \frac{1}{N}\mathcal{G}_{ii}(t,t)/i\right] - r_0^2\right\} \tag{23}$$

$$-\frac{\delta\Gamma[x]}{\delta x_i(t)} = \left\{\frac{\mathrm{d}^2}{\mathrm{d}t^2} + \chi(t)\right\} x_i(t) + \frac{1}{N}\mathcal{K}_i(t,t)/i \, . \tag{24}$$

However the Green's functions here, $\mathcal{G}_{ii}(t,t)$ and $\mathcal{K}_i(t,t)$ are defined in Eq. (21) as functionals of the currents $j_\alpha(t)$. These must be expressed as functionals of $x_\alpha(t)$ by inverse relations. We define these inverse Green's functions, which are functionals of $x_\alpha(t)$, by:

$$\mathcal{G}^{-1}_{\alpha,\beta}[x](t,t') = \frac{\delta j_\alpha(t)}{\delta x_\beta(t')} = -\frac{\delta^2\Gamma[x]}{\delta x_\alpha(t)\,\delta x_\beta(t')} = \begin{pmatrix} \mathcal{D}^{-1}(t,t') & \bar{\mathcal{K}}^{-1}_j(t,t') \\ \mathcal{K}^{-1}_i(t,t') & \mathcal{G}^{-1}_{i,j}(t,t') \end{pmatrix} \, , \tag{25}$$

where explicitly

$$\mathcal{D}^{-1}(t,t') = -\frac{\delta^2\Gamma[\chi,x]}{\delta\chi(t)\,\delta\chi(t')} \qquad \bar{\mathcal{K}}^{-1}_i(t,t') = -\frac{\delta^2\Gamma[\chi,x]}{\delta\chi(t)\,\delta x_i(t')}$$
$$\mathcal{K}^{-1}_i(t,t') = -\frac{\delta^2\Gamma[\chi,x]}{\delta x_i(t)\,\delta\chi(t')} \qquad \mathcal{G}^{-1}_{i,j}(t,t') = -\frac{\delta^2\Gamma[\chi,x]}{\delta x_i(t)\,\delta x_j(t')} \, .$$

Again we have $\bar{\mathcal{K}}^{-1}_i(t,t') = \mathcal{K}^{-1}_i(t',t)$. The inverse Green's functions are given by differentiating the equations of motion, Eqs. (23) and (24), with respect to the coordinates. Using

$$\int_{\mathcal{C}} \mathrm{d}t' \sum_{\beta} \mathcal{G}^{-1}_{\alpha,\beta}[x](t,t')\,\mathcal{G}_{\beta,\gamma}[j](t',t'') = \delta_{\alpha,\gamma}\delta_{\mathcal{C}}(t,t'') \, , \tag{26}$$

we find:

$$\frac{\delta\mathcal{G}_{\alpha,\beta}[j](t_1,t_2)}{\delta x_\gamma(t_3)} = -\int_{\mathcal{C}} \mathrm{d}t_4 \int_{\mathcal{C}} \mathrm{d}t_5 \sum_{\delta,\epsilon} \mathcal{G}_{\alpha,\delta}[j](t_1,t_4)\,\Gamma_{\delta,\epsilon,\gamma}[x](t_4,t_5,t_3)\,\mathcal{G}_{\epsilon,\beta}[j](t_5,t_2) \, , \tag{27}$$

where $\Gamma_{\alpha,\beta,\gamma}[x](t_1,t_2,t_3)$ is the three-point vertex function, defined by:

$$\Gamma_{\alpha,\beta,\gamma}[x](t_1,t_2,t_3) = \frac{\delta\mathcal{G}^{-1}_{\alpha,\beta}[x](t_1,t_2)}{\delta x_\gamma(t_3)} = -\frac{\delta^3\Gamma[x]}{\delta x_\alpha(t_1)\,\delta x_\beta(t_2)\,\delta x_\gamma(t_3)} \, . \tag{28}$$

Explicitly, we find an equation of the form:

$$\mathcal{G}^{-1}_{\alpha,\beta}(t,t') = G^{-1}_{\alpha,\beta}(t,t') + \Sigma_{\alpha,\beta}(t,t') \,, \tag{29}$$

where $G^{-1}_{\alpha,\beta}(t,t')$ is given by Eq. (17). The generalized self energy $\Sigma_{\alpha,\beta}(t,t')$ is given by:

$$\Sigma_{\alpha,\beta}(t,t') = \begin{pmatrix} \Pi(t,t') & \Omega_j(t,t') \\ \bar{\Omega}_i(t,t') & \Sigma_{ij}(t,t') \end{pmatrix} \,, \tag{30}$$

and where the polarization $\Pi(t,t')$, self energy $\Sigma_{ij}(t,t')$, and the off diagonal terms $\Lambda_i(t,t')$ and $\bar{\Lambda}_i(t,t')$ are given by:

$$\begin{aligned}
\Pi(t,t') &= \frac{i}{2N} \sum_{i,\alpha,\beta} \int_{\mathcal{C}} \mathrm{d}t_1 \int_{\mathcal{C}} \mathrm{d}t_2 \, \mathcal{G}_{i,\alpha}(t,t_1) \Gamma_{\alpha,\beta,0}(t_1,t_2,t') \mathcal{G}_{\beta,i}(t_2,t) \,, \\
\Sigma_{ij}(t,t') &= \frac{i}{N} \sum_{\alpha,\beta} \int_{\mathcal{C}} \mathrm{d}t_1 \int_{\mathcal{C}} \mathrm{d}t_2 \, \mathcal{G}_{i,\alpha}(t,t_1) \, \Gamma_{\alpha,\beta,j}(t_1,t_2,t') \mathcal{G}_{\beta,0}(t_2,t) \\
\Omega_i(t,t') &= \frac{i}{2N} \sum_{j,\alpha,\beta} \int_{\mathcal{C}} \mathrm{d}t_1 \int_{\mathcal{C}} \mathrm{d}t_2 \, \mathcal{G}_{j,\alpha}(t,t_1) \Gamma_{\alpha,\beta,i}(t_1,t_2,t') \mathcal{G}_{\beta,j}(t_2,t) \\
\bar{\Omega}_i(t,t') &= \frac{i}{N} \sum_{\alpha\beta} \int_{\mathcal{C}} \mathrm{d}t_1 \int_{\mathcal{C}} \mathrm{d}t_2 \, \mathcal{G}_{i,\alpha}(t,t_1) \Gamma_{\alpha,\beta,0}(t_1,t_2,t') \mathcal{G}_{\beta,0}(t_2,t) \,.
\end{aligned} \tag{31}$$

In order to solve the equation for the two point function, Eq. (29), one requires knowledge of the three point function, defined by Eq. (28). This in turn requires knowledge of the four-point function, *ad infinitum*. It is this infinite hierarchy of coupled Green's function equations that corresponds to solving exactly the Schrödinger equation.

The matrix inversion of Eq. (29) gives the set of coupled equations,

$$\mathcal{G}_{\alpha,\beta}(t,t') = G_{\alpha,\beta}(t,t') - \sum_{\gamma,\delta} \int_{\mathcal{C}} \mathrm{d}t_1 \int_{\mathcal{C}} \mathrm{d}t_2 \, G_{\alpha,\gamma}(t,t_1) \, \Sigma_{\gamma,\delta}(t_1,t_2) \, \mathcal{G}_{\delta,\beta}(t_2,t') \,, \tag{32}$$

where

$$G_{\alpha,\beta}(t,t') = \begin{pmatrix} D(t,t') & K_i(t,t') \\ \bar{K}_i(t,t') & G_{ij}(t,t') \end{pmatrix} \,. \tag{33}$$

with

$$\sum_j \left\{ \left[\frac{\mathrm{d}^2}{\mathrm{d}t^2} + \chi(t) \right] \delta_{ij} + g \, x_i(t) \, x_j(t) \right\} G_{jk}(t,t') = \delta_{ik} \, \delta_{\mathcal{C}}(t,t') \,, \tag{34}$$

$$D(t,t') = -g \, \delta_{\mathcal{C}}(t,t') + g^2 \sum_{ij} x_i(t) \, G_{ij}(t,t') \, x_j(t') \,, \tag{35}$$

$$\bar{K}_j(t,t') = K_j(t',t) = g \sum_i G_{ji}(t,t') \, x_i(t') \,. \tag{36}$$

When $x_i(t) \neq 0$, one notes that $D(t,t')$ is not the inverse of $D^{-1}(t,t')$.

The vertex function $\Gamma_{\alpha,\beta,\gamma}[x](t_1,t_2,t_3)$ defined in Eq. (28) is obtained by differentiation of Eq. (29) with respect to $x_\gamma(t)$. We find:

$$\begin{aligned}\Gamma_{\alpha,\beta,\gamma}[x](t_1,t_2,t_3) &= \frac{\delta \mathcal{G}^{-1}_{\alpha,\beta}[x](t_1,t_2)}{\delta x_\gamma(t_3)} \\ &= f_{\alpha,\beta,\gamma}\,\delta_{\mathcal{C}}(t_1,t_2)\,\delta_{\mathcal{C}}(t_1,t_3) + \Phi_{\alpha,\beta,\gamma}[x](t_1,t_2,t_3)\,. \end{aligned} \tag{37}$$

Here $f_{i,j,0} = f_{0,i,j} = f_{i,0,j} = \delta_{ij}$, otherwise f is zero. $\Phi_{\alpha,\beta,\gamma}[x](t_1,t_2,t_3)$ is given by derivatives of the self-energy matrix:

$$\Phi_{\alpha,\beta,\gamma}[x](t_1,t_2,t_3) = \frac{\delta\,\Sigma_{\alpha,\beta}[x](t_1,t_2)}{\delta x_\gamma(t_3)}\,, \tag{38}$$

and is of order $1/N$.

We are interested in resummation schemes that are exact to order $1/N$ for $\langle x_i^2 \rangle$. We see from Eqs. (37) and (38) that it is consistent to replace $\Gamma_{\alpha,\beta,\gamma}[x](t_1,t_2,t_3)$ in Eq. (32) by the first term in Eq. (37) to obtain a resummation which is exact to order $1/N$. To simplify our discussion of the exact Schwinger-Dyson equation for the vertex function, we will only consider the case of the quantum roll where $x_i(t) = 0$.

Following the treatment of ref. [14] we have for the 3-χ vertex:

$$\Lambda(t_1,t_2,t_3) = \frac{\delta \mathcal{D}^{-1}(t_1,t_2)}{\delta\chi(t_3)} = \int_{\mathcal{C}} \mathrm{d}t_4 \int_{\mathcal{C}} \mathrm{d}t_5\, \mathcal{G}_{ij}(t_1,t_4)\, M_{jk}(t_4,t_5;t_2,t_3)\, \mathcal{G}_{ki}(t_5,t_1) \tag{39}$$

where $M_{jk}(t_4,t_5;t_2,t_3)$ is 1-PI in the channel $x + x \rightarrow \chi + \chi$. The lowest order in $1/N$ contribution to $M(t_4,t_5;t_2,t_3)$ is:

$$M_{jk}(t_4,t_5;t_2,t_3) = \delta(t_4 - t_2)\delta(t_5 - t_3)\,\mathcal{G}_{jk}(t_2,t_3)\,. \tag{40}$$

When $x_i(t) = 0$, the exact Schwinger-Dyson equation for the χ-x-x vertex is

$$\Gamma(t_1,t_2,t_3) = \delta\mathcal{G}^{-1}(t_1,t_2)\delta\chi(t_3) = 1 + i\Gamma\mathcal{G}K_1\mathcal{G} + i\Lambda_3\mathcal{D}\,K_2\,\mathcal{D} \tag{41}$$

where K_1 and K_2 are the s-channel 2-PI scattering amplitudes for the reactions: $x+x \rightarrow x+x$ and $\chi + \chi \rightarrow x + x$, respectively.

This is shown pictorially in Fig. 1. In general one then has to obtain equations for the 2-PI scattering amplitudes as well as for Λ. These will depend on even higher n-point functions, *ad infinitum*. In our approximations made at the two-point function level, the 2-PI s-channel scattering amplitudes K_1 and K_2, used in the equations for the vertex function, will turn out to be graphs for one-particle exchange in the t-channel of the χ- and x-particles respectively.

In our truncations of the Schwinger-Dyson equations, we will replace the full 3-point vertex function by the bare one in the equations for x and $\mathcal{G}$ in the *presence* of external sources. However one still gets a non-trivial equation for the vertex function in the *absence* of sources in these approximations by functionally differentiating the equation for the inverse two-point function with respect to the coordinate. The bare vertex approximation is found by this procedure. The other two approximations we will consider consist of further approximations to the one- and two-point functions.

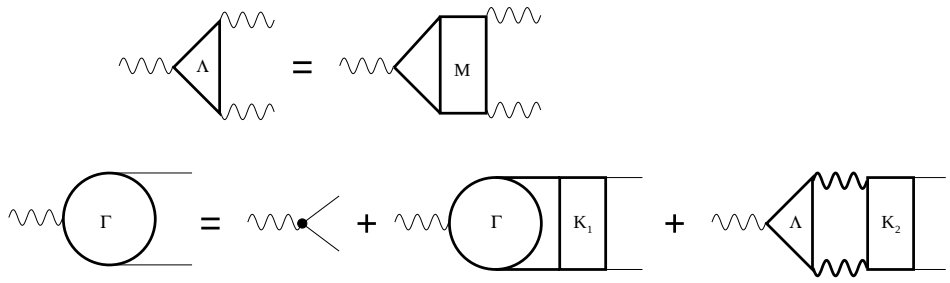

Figure 1: Schwinger-Dyson equations for the vertex function. Solid lines represent the $\mathcal{G}_{ij}(t,t')$ propagator and heavy wiggly lines are the $\mathcal{D}(t,t')$ propagator.

4 Effective action for two-particle irreducible graphs

Since the approximations we are going to consider have a simple interpretation in terms of keeping a particular 2-PI vacuum graph in the generating functional of the 2-PI graphs, we would like to review this formalism following the approach of Cornwall, Jackiw, and Tomboulis (CJT)[15].

The first Legendre transform of the generating functional $W[j]$ of connected Green's functions is widely known and used and is called the "effective action." The higher Legendre transforms (second, third, etc.) were introduced by De Dominicis and Martin[16] in quantum statistics. Dahmen and Jona-Lasinio[17], and later Visil'ev and Kazanskii[18], extended these ideas to quantum field theory. These methods were then used by Cornwall, Jackiw, and Tomboulis to discuss dynamical symmetry breaking in Hartree type approximations which later led to the second Legendre transformation formalism being called the CJT formalism. These higher order Legendre transformed actions have the advantage of being able to treat higher order Green's functions on the same footing as the coordinates.

We will first summarize the general results of that paper before proceeding to the specific approximations we consider in this paper. The method of CJT is to introduce one- and two-body sources for the coordinates $x_\alpha(t)$ and the Green's functions $\mathcal{G}_{\alpha,\beta}(t,t')$ in the action, and then make a Legendre transformation to the one- and two-point functions. The resulting action, as a function of x and $\mathcal{G}$, contains a term which is the sum of all two-particle irreducible vacuum graphs. This term can be written using the vertices of the interaction and $\mathcal{G}$. We use the extended notation for the coordinates and one-body sources, given in Eq. (11).

Thus, the generating functional $Z[j,k]$ for the CJT action is given by:

$$Z[j,k] = e^{iNW[j,k]} = \prod_{\alpha=0}^{N} \int \mathrm{d}x_\alpha \, \exp\left\{iNS_N[x;j,k]\right\} \ , \tag{42}$$

with

$$S_N[x;j,k] = S_{\rm class}[x] + \sum_\alpha \int_{\mathcal{C}} {\rm d}t\, x_\alpha(t)\, j_\alpha(t) + \frac{1}{2}\sum_{\alpha,\beta}\int_{\mathcal{C}}{\rm d}t\int_{\mathcal{C}}{\rm d}t'\, x_\alpha(t)\, k_{\alpha,\beta}(t,t')\, x_\beta(t')\;, \quad (43)$$

where

$$S_{\rm class}[x] = -\frac{1}{2}\sum_{\alpha,\beta}\int_{\mathcal{C}}{\rm d}t\int_{\mathcal{C}}{\rm d}t'\, x_\alpha(t)\,\Delta^{-1}_{\alpha,\beta}[x](t,t')\, x_\beta(t') = S_0 + S_{\rm int}[x]\;, \quad (44)$$

$$S_0 = -\frac{1}{2}\sum_{\alpha,\beta}\int_{\mathcal{C}}{\rm d}t\int_{\mathcal{C}}{\rm d}t'\, x_\alpha(t)\,\Delta^{-1}_{0\,\alpha,\beta}(t,t')\, x_\beta(t')\;, \quad (45)$$

$$S_{\rm int}[x] = -\frac{1}{2}\int_{\mathcal{C}}{\rm d}t\,\chi(t)\sum_i x_i^2(t)\;, \quad (46)$$

and where $\Delta^{-1}_{0\,\alpha,\beta}(t,t')$ is given by:

$$\Delta^{-1}_{0\,\alpha,\beta}(t,t') = \begin{pmatrix} D^{-1}(t,t') & 0 \\ 0 & G^{-1}_{0\,ij}(t,t') \end{pmatrix}\;, \quad (47)$$

with $D^{-1}(t,t')$ given by Eq. (15), and $G^{-1}_{0\,ij}(t,t')$ defined by:

$$G^{-1}_{0\,ij}(t,t') = \left\{\frac{{\rm d}^2}{{\rm d}t^2}\right\}\delta_{ij}\delta_{\mathcal{C}}(t,t')\;. \quad (48)$$

In this formalism, we have separated out an "interaction" term, Eq. (46), which depends on the coordinates $x_\alpha(t)$, from a bare Green's function $G^{-1}_{0\,ij}(t,t')$, *which is independent of the coordinates* $x_\alpha(t)$, in contrast to our previous definitions in Eq. (16). The term $r_0^2\chi(t)/2$ has been absorbed into the definition of the current $\tilde{J}(t)$ in Eq. (11).

The second Legendre transform of $W[j,k]$ is the CJT effective action:

$$\Gamma[x,\mathcal{G}] = W[j,k] - \sum_\alpha\int_{\mathcal{C}}{\rm d}t\, x_\alpha(t)\, j_\alpha(t) + \frac{1}{2}\sum_{\alpha,\beta}\int_{\mathcal{C}}{\rm d}t\int_{\mathcal{C}}{\rm d}t'\, k_{\alpha,\beta}(t,t')\,\left\{x_\alpha(t)\, x_\beta(t') + \mathcal{G}_{\alpha,\beta}(t,t')\right\}\;. \quad (49)$$

CJT showed that $\Gamma[x,\mathcal{G}]$ can be obtained as a series expansion in terms of 2-PI graphs. That is, introducing the functional operator,

$$G^{-1}_{\alpha,\beta}[x](t,t') = -\frac{\delta^2 S_0[x]}{\delta x_\alpha(t)\,\delta x_\beta(t')} = \begin{pmatrix} D^{-1}(t,t') & \bar{K}^{-1}_j[x](t,t') \\ K^{-1}_i[x](t,t') & G^{-1}_{i,j}[x](t,t') \end{pmatrix}\;, \quad (50)$$

which is the same as the $G^{-1}_{\alpha,\beta}[x](t,t')$ as defined in Eq. (17), one can write the effective action in the form:

$$\Gamma[x,\mathcal{G}] = S_{\rm class}[x] + \frac{i}{2}{\rm Tr}\{\ln[\,\mathcal{G}^{-1}\,]\} + \frac{i}{2}{\rm Tr}\{G^{-1}[x]\,\mathcal{G} - 1\} + \Gamma_2[x,\mathcal{G}]\;. \quad (51)$$

The quantity $\Gamma_2[x,\mathcal{G}]$ has a simple graphical interpretation in terms of all the 2-PI vacuum graphs using vertices from the interaction term. The Hartree and leading order in large-N approximation for the x^4 potential was obtained by CJT using a single two-loop vacuum graph in the $O(N)$ theory written in terms of only the coordinates x_i. Our strategy for obtaining a resummation of the large-N approximation is to first rewrite the theory in terms of the composite field χ, and the equivalent Lagrangian given in Eq. (10). Using these new variables, we then choose for $\Gamma_2[x,\mathcal{G}]$ the 2-PI graphs shown in Fig. 3, which is now written in terms of the full χ and x propagators and the trilinear coupling $\chi(t)\,x_i^2(t)/2$.

5 Bare Vertex Approximation

The most robust approximation we will consider here is to set the vertex function equal its bare value in the exact equations for the one and two point functions. This is an energy conserving approximation which leads to integral eqution for the three-χ vertex function as well as for the x-x-χ vertex function. The bare vertex approximation consists of making the replacement

$$\Gamma_{\alpha,\beta,\gamma}[x](t_1,t_2,t_3) = f_{\alpha,\beta,\gamma}\,\delta_{\mathcal{C}}(t_1,t_2)\,\delta_{\mathcal{C}}(t_1,t_3)\,. \tag{52}$$

in the exact Schwinger-Dyson equations for the self-energies, Eqs. (31). This gives for the BVA:

$$\begin{aligned}
\Pi(t,t') &= \frac{i}{2N}\sum_{ij}\mathcal{G}_{ij}(t,t')\,\mathcal{G}_{ji}(t',t)\,,\\
\Sigma_{ij}(t,t') &= \frac{i}{N}\left\{\bar{\mathcal{K}}_i(t,t')\,\mathcal{K}_j(t',t) + \mathcal{G}_{ij}(t,t')\,\mathcal{D}(t',t)\right\},\\
\Omega_i(t,t') &= \frac{i}{N}\sum_j \bar{\mathcal{K}}_j(t,t')\,\mathcal{G}_{ji}(t,t')\\
\bar{\Omega}_i(t,t') &= \frac{i}{N}\sum_j \mathcal{K}_j(t',t)\,\mathcal{G}_{ji}(t',t)
\end{aligned} \tag{53}$$

where we have used the symmetry property, $\mathcal{G}_{ij}(t,t') = \mathcal{G}_{ji}(t',t)$ and $\mathcal{K}_i(t,t') = \bar{\mathcal{K}}_i(t',t)$. Thus we find $\bar{\Omega}_i(t,t') = \Omega_i(t',t)$. The self-energies (53) are then used in Eqs. (29) to find the one- and two-point functions. For the Green's functions, we find:

$$\mathcal{G}^{-1}_{\alpha,\beta}(t,t') = G^{-1}_{\alpha,\beta}(t,t') + \Sigma_{\mathrm{BVA}\,\alpha,\beta}(t,t')\,, \tag{54}$$

with $\Sigma_{\mathrm{BVA}\,\alpha,\beta}(t,t')$ given by Eq. (53). The inversion of Eq. (54) is given by Eq. (32), which is a set of four coupled integral equations for the four BVA Green's functions, which must be solved simultaniously. From Eqs. (23) and (24), the equations of motion for $x_i(t)$ and the

gap equation for $\chi(t)$ is then given by:

$$\left\{\frac{\mathrm{d}^2}{\mathrm{d}t^2}+\chi(t)\right\}x_i(t)+\frac{1}{N}\mathcal{K}_i(t,t)/i=0\,, \tag{55}$$

$$\chi(t)=\frac{g}{2}\left\{\sum_i\left[x_i^2(t)+\frac{1}{N}\mathcal{G}_{ii}(t,t)/i\right]-r_0^2\right\}. \tag{56}$$

For the quantum roll, we further set $x_i(t)=0$. This means that $\mathcal{K}_i(t,t)=\bar{\mathcal{K}}_i(t,t)=0$, so that $G_{\alpha\beta}(t,t')$ is diagonal, and results in the following set of equations for the Green's functions:

$$\mathcal{D}(t,t')=D(t,t')-\int_{\mathcal{C}}\mathrm{d}t_1\int_{\mathcal{C}}\mathrm{d}t_2\,D(t,t_1)\,\Pi(t_1,t_2)\,\mathcal{D}(t_2,t')\,, \tag{57}$$

$$\mathcal{G}_{ij}(t,t')=G_{ij}(t,t')-\sum_{kl}\int_{\mathcal{C}}\mathrm{d}t_1\int_{\mathcal{C}}\mathrm{d}t_2\,G_{ik}(t,t_1)\,\Sigma_{kl}(t_1,t_2)\,\mathcal{G}_{lj}(t_2,t')\,, \tag{58}$$

where

$$\Pi(t,t')=\frac{i}{2N}\sum_{ij}\mathcal{G}_{ij}(t,t')\,\mathcal{G}_{ji}(t',t)\,,\qquad \Sigma_{ij}(t,t')=\frac{i}{N}\,\mathcal{G}_{ij}(t,t')\,\mathcal{D}(t',t)\,. \tag{59}$$

The gap equation for $\chi(t)$ becomes:

$$\chi(t)=\frac{g}{2}\left\{\frac{1}{N}\sum_i\mathcal{G}_{ii}(t,t)/i-r_0^2\right\}. \tag{60}$$

In addition, for this case, the initial conditions imply that we can take $G_{ij}(t,t')$ and $\mathcal{G}_{ij}(t,t')$ to be diagonal, which greatly simplify the integral equations. The BVA for the quantum roll requires that we solve equations (57), (58), (59), and (60) simultaneously using the numerical methods described in refs. [20] and [21].

The three-point vertex functions $\Lambda(t_1,t_2,t_3)$ and $\Gamma_{ij}(t_1,t_2,t_3)$ for the BVA is given by:

$$\Lambda(t_1,t_2,t_3)\equiv\Gamma_{000}(t_1,t_2,t_3)=\frac{\delta\,\mathcal{D}^{-1}(t_1,t_2)}{\delta\chi(t_3)} \tag{61}$$

$$\Gamma_{ij}(t_1,t_2,t_3)\equiv\Gamma_{ij0}(t_1,t_2,t_3)=\frac{\delta\,\mathcal{G}_{ij}^{-1}(t_1,t_2)}{\delta\chi(t_3)}\,, \tag{62}$$

and obtain the coupled integral equations:

$$\Lambda(t_1,t_2,t_3)=-\frac{i}{N}\int_{\mathcal{C}}\mathrm{d}t_4\int_{\mathcal{C}}\mathrm{d}t_5\sum_{ijkl}\mathcal{G}_{ik}(t_1,t_4)\,\Gamma_{kl}(t_4,t_5,t_3)\,\mathcal{G}_{lj}(t_5,t_2)\,\mathcal{G}_{ji}(t_2,t_1) \tag{63}$$

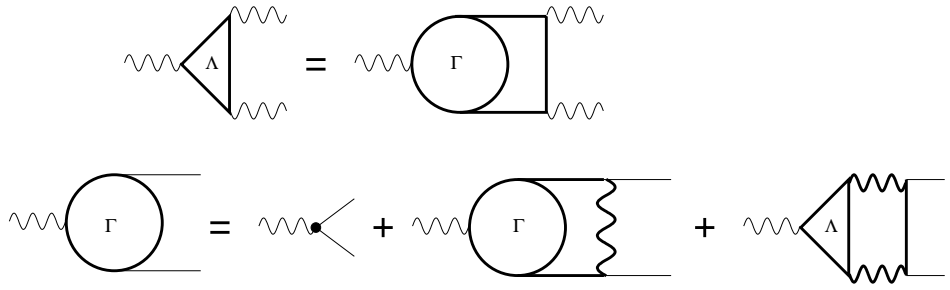

Figure 2: The Vertex equations for the BVA. The top figure represents Eq. (63) and the bottom figure represents Eq. (64). Solid lines represent the $\mathcal{G}_{ij}(t,t')$ propagator and heavy wiggly lines are the $\mathcal{D}(t,t')$ propagator.

and

$$\Gamma_{ij}(t_1,t_2,t_3) = \delta_{\mathcal{C}}(t_1,t_2)\,\delta_{\mathcal{C}}(t_1,t_3) - \int_{\mathcal{C}} \mathrm{d}t_4 \int_{\mathcal{C}} \mathrm{d}t_5 \Big\{ \sum_{kl} \mathcal{G}_{ik}(t_1,t_4)\,\Gamma_{kl}(t_4,t_5,t_3)\,\mathcal{G}_{lj}(t_5,t_2)\,\mathcal{D}(t_2,t_1) + \mathcal{G}_{ij}(t_1,t_2)\mathcal{D}(t_2,t_4)\,\Lambda(t_4,t_5,t_3)\,\mathcal{D}(t_5,t_1) \Big\}. \quad (64)$$

This is shown diagramatically in Fig. 2. Looking at the diagrams, if we iterate these equations, we sum all the "rainbow" diagrams. As advertized, comparing these graphs with those shown in Fig. 1, K_1 is approximated in the BVA by χ exchange and K_2 by x exchange in the t-channel.

Let us show that this approximation is easy to obtain from the CJT formalism once we treat $\mathcal{G}$ and $\mathcal{D}$ and $\mathcal{K}$ on exactly the same footing. We choose for our approximation to $\Gamma_2[\mathcal{G}]$

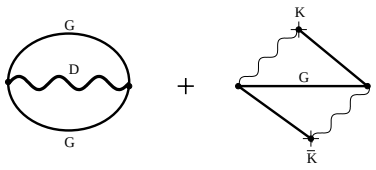

Figure 3: Self-energy diagrams for the two-point function $\Gamma_2[\mathcal{G}]$. Solid lines represent the $\mathcal{G}_{ij}(t,t')$ propagator, the wiggly to solid lines represent the $\mathcal{K}_i(t,t')$ and $\bar{\mathcal{K}}_i(t,t')$ propagator, and wiggly lines are the $\mathcal{D}(t,t')$ propagator.

the 2-PI graphs shown in Fig. 3. This gives:

$$\Gamma_2[\mathcal{G}] = -\frac{1}{4N}\sum_{ij}\int_{\mathcal{C}} \mathrm{d}t_1 \int_{\mathcal{C}} \mathrm{d}t_2\, \mathcal{D}(t_1,t_2)\, \mathcal{G}_{ij}(t_1,t_2)\, \mathcal{G}_{ji}(t_2,t_1)$$
$$- \frac{1}{2N}\sum_{ij}\int_{\mathcal{C}} \mathrm{d}t_1 \int_{\mathcal{C}} \mathrm{d}t_2\, \bar{\mathcal{K}}_i(t_1,t_2)\, \mathcal{G}_{ij}(t_1,t_2)\, \mathcal{K}_j(t_2,t_1)\,. \tag{65}$$

The CJT action is given by Eq. (51). The stationary condition for $\mathcal{G}_{\alpha,\beta}(t,t')$ gives:

$$\frac{\delta\Gamma[x,\mathcal{G}]}{\delta\mathcal{G}_{\alpha\beta}} = \frac{i}{2}\left\{G^{-1}_{\alpha\beta}[x] - \mathcal{G}^{-1}_{\alpha\beta}\right\} + \frac{\delta\Gamma_2[\mathcal{G}]}{\delta\mathcal{G}_{\alpha\beta}} = 0\,,$$
$$\text{or} \qquad \mathcal{G}^{-1}_{\alpha,\beta}(t,t') = G^{-1}_{\alpha,\beta}(t,t') + \Sigma_{\mathrm{BVA}\,\alpha,\beta}[\mathcal{G}](t,t')\,,$$
$$\text{where:} \qquad \Sigma_{\mathrm{BVA}\,\alpha,\beta}[\mathcal{G}](t,t') = -2i\,\frac{\delta\Gamma_2[\mathcal{G}]}{\delta\mathcal{G}_{\alpha\beta}}\,. \tag{66}$$

Carrying out the derivatives of $\Gamma_2[\mathcal{G}]$ given in Eq. (65), we find that $\Sigma_{\mathrm{BVA}\,\alpha,\beta}(t,t')$ is exactly the same as found in Eq. (53) using the Schwinger-Dyson equations in the BVA approximation. The stationary condition for x_α also gives the same equations of motion for $x_i(t)$ and gap equation for $\chi(t)$ as found in Eqs. (55) and (56) using the Schwinger-Dyson equations in the BVA. Thus we conclude that the CJT action, as given in Eqs. (51) and (65), gives exactly the same set of equations as in the Schwinger-Dyson BVA truncation.

The fact that the BVA equations are derivable from an effective action ensures energy conservation. To get the effective action as a function of x_i only, one needs to first solve

$$\delta\Gamma[x_i,\chi]\delta\chi = 0$$

to obtain $\chi = \chi(x_i)$, and then find $\Gamma[x_i] = \Gamma[x_i,\chi(x_i)]$. The standard effective potential, $V_{\mathrm{eff}}(x_i)$, is the static part of this action.

6 Dynamical Debye Screening Approximation

In plasma studies of the electric conductivity of fully ionized plasmas [9, 10], it was found that in order to correctly determine the conductivity it was neccesary to have an approximation where the photon propagator included the effects of dynamical Debye screening in the random phase approximation. This improved propagator was then used in a scattering kernel in the kinetic equations. In our model, the χ field plays the roll of the photon in the dynamics of the x_i oscillators. The lowest approximation that includes the polarization effects in $\mathcal{D}$ is precisely the leading order in large-N approximation to $\mathcal{D}$, namely D. The leading order in large-N approximation is similar in spirit to the random phase approximation. The equation for $\mathcal{D}^{-1}(t,t')$ in leading order in large-N is given by (see below):

$$\mathcal{D}_0^{-1}(t,t') = -\frac{1}{g}\delta_{\mathcal{C}}(t,t') + \Pi_0(t,t')\,, \tag{67}$$

where

$$\Pi_0(t,t') = \frac{i}{2N}\sum_{i,j} G_{ij}(t,t')\,G_{ji}(t',t) + \sum_{i,j} x_i(t)\,G_{ij}(t,t')\,x_j(t')\,. \tag{68}$$

Let us now specialize to the case when $x_i(t) = 0$. The equation for the full x propagator $\mathcal{G}$ is:

$$\mathcal{G}_{ij}(t,t') = G_{ij}(t,t') - \sum_{k,l}\int_{\mathcal{C}} \mathrm{d}t_1 \int_{\mathcal{C}} \mathrm{d}t_2\, G_{ik}(t,t_1)\,\Sigma_{kl}(t_1,t_2)\,\mathcal{G}_{lj}(t_2,t')\,, \tag{69}$$

with the self energy depending on the full $\mathcal{G}$ and the leading order in $1/N$ approximation to $\mathcal{D}$ given by Eq. (67):

$$\Sigma_{kl}(t,t') = \frac{i}{N}\,\mathcal{G}_{kl}(t,t')\,D(t,t')\,. \tag{70}$$

The gap equation is:

$$\chi(t) = \frac{g}{2}\,\left\{\sum_i \frac{1}{N}\mathcal{G}_{ii}(t,t)/i - r_0^2\right\}\,. \tag{71}$$

There is a nontrivial vertex function in this approximation given by:

$$\begin{aligned}\Gamma_{ij}(t_1,t_2,t_3) &= \frac{\delta\mathcal{G}^{-1}_{ij}[\chi](t_1,t_2)}{\delta\chi(t_3)} \\ &= \delta_{\mathcal{C}}(t_1,t_2)\delta_{\mathcal{C}}(t_3,t_2)\delta_{ij} - \sum_{kl}\int_{\mathcal{C}}\mathrm{d}t_4\int_{\mathcal{C}}\mathrm{d}t_5\,\Gamma_{kl}(t_4,t_5,t_3)\,\mathcal{G}_{ki}(t_4,t_1)\,D(t_1,t_2)\,\mathcal{G}_{jl}(t_2,t_5) \\ &\qquad - \int_{\mathcal{C}}\mathrm{d}t_4\int_{\mathcal{C}}\mathrm{d}t_5\,\Lambda(t_4,t_5,t_3)\,D(t_4,t_1)\,\mathcal{G}_{ij}(t_1,t_2)\,D(t_2,t_5)\,.\end{aligned} \tag{72}$$

This equation can be obtained from the exact integral equation for Γ shown pictorially in Fig. 1 by making two approximations. The first is to approximate the exact 3-χ vertex function by the triangle graph, which is the leading term in the $1/N$ expansion of this function. The second is to replace the scattering kernals, K_1 and K_2 by single particle exchange in the t-channel.

The DDSA approximation can be derived from an effective action by modifying slightly the approach of Cornwall, Jackiw and Tomboulis (CJT) [15]. The discussion that follows here is due to Emil Mottola and Luis Bettencourt [19]. Thinking of the fields x and χ as part of an $N+1$ component field, and considering the case that $\langle x\rangle = 0$, so that there is no mixed propagator, one can write a CJT like action for the generating functional of the twice Legendre transformed effective action as:

$$\begin{aligned}\Gamma[\chi,\mathcal{G},\mathcal{D}] = S_{\text{class}}[\chi] &+ \frac{i}{2}\mathrm{Tr}\{\ln[\,\mathcal{D}^{-1}\,]\} + \frac{i}{2}\mathrm{Tr}\{\ln[\,\mathcal{G}^{-1}\,]\} \\ &+ \frac{i}{2}\mathrm{Tr}\{D^{-1}[\chi]\,\mathcal{D} + G^{-1}[\chi]\,\mathcal{G} - 1\} + \Gamma_2[\mathcal{G}]\,.\end{aligned} \tag{73}$$

here the quantites $G^{-1}(t,t')$ and $D^{-1}(t,t')$ are defined in Eqs. (15) and (16). In the DDSA, the 2-PI contribution to the action, $\Gamma_2[\mathcal{G}]$, for the case when $x_i(t) = 0$, is given by Eq. (65) with $\mathcal{D}(t,t')$ set equal to the first order result $D(t,t')$:

$$\Gamma_2[\mathcal{G}] = -\frac{1}{4N}\sum_{ij}\int_{\mathcal{C}} \mathrm{d}t_1 \int_{\mathcal{C}} \mathrm{d}t_2\, D(t_1,t_2)\,\mathcal{G}_{ij}(t_1,t_2)\,\mathcal{G}_{ji}(t_2,t_1)\,. \tag{74}$$

Here $D(t,t')$ is considered to be an external variable and not varied! By varying this action, we reproduce Eqs. (69) and (71). Although there is an effective action for the DDSA approximation, since D is considered an external time-dependent propagator, energy is not conserved in this approximation.

7 The large-N approximation

The large-N expansion is obtained from Eq. (12) by first integrating over all the x_i and then evaluating the remaining functional integral over χ by steepest descent. The effective action, as a power series in $1/N$, is obtained from the first Legendre transform of the generating functional. In a previous paper[6], we obtained equations for the next to leading order large-N approximation to the action, and gave numerical results for the quantum roll, comparing our approximation to exact solutions. For completeness, we review those equations here. To order $1/N$, we obtain:

$$\Gamma_{\text{Large-N}}[x] = S_{\text{class}}[x] + \int_{\mathcal{C}} \mathrm{d}t \left\{ \frac{i}{2}\sum_i \ln\left[G_{ii}^{-1}(t,t)\right] + \frac{i}{2N}\ln[\mathcal{D}_0^{-1}(t,t)] \right\}, \tag{75}$$

where $S_{\text{class}}[x]$ is given by Eq. (44), and $\mathcal{D}_0^{-1}(t,t')$ is the inverse propagators for χ in lowest order in the $1/N$ expansion, given by

$$\mathcal{D}_0^{-1}(t,t') = D^{-1}(t,t') + \Pi_0(t,t')\,,$$

with

$$\Pi_0(t,t') = \frac{i}{2N}\sum_{i,j} G_{ij}(t,t')\,G_{ji}(t',t) - \sum_{i,j} x_i(t)\,G_{ij}(t,t')\,x_j(t')\,. \tag{76}$$

Here $D^{-1}(t,t')$ and $G_{ij}^{-1}(t,t')$ are the same as Eqs. (15) and (16) that we defined earlier.

The equations of motion for the classical fields $x_i(t)$, to next to leading order in $1/N$, are given by:

$$\left\{\frac{\mathrm{d}^2}{\mathrm{d}t^2} + \chi(t)\right\} x_i(t) + i\sum_j \int_{\mathcal{C}} \mathrm{d}t'\, G_{ij}(t,t')\,\mathcal{D}_0(t,t')\,x_j(t') = 0\,, \tag{77}$$

with the gap equation for $\chi(t)$ given by

$$\chi(t) = \frac{g}{2}\left\{\sum_i \left(x_i^2(t) + \frac{1}{N}\sum_i \mathcal{G}^{(2)}_{ii}(t,t)/i\right) - r_0^2\right\}\,, \tag{78}$$

and where the second order x_i propagator $\mathcal{G}^{(2)}_{ij}(t,t)$ and self energy $\Sigma_{ij}(t,t')$ to order $1/N$ is given by

$$\begin{aligned}
\mathcal{G}^{(2)}_{ij}(t,t') &= G_{ij}(t,t') - \sum_{k,l}\int_{\mathcal{C}} \mathrm{d}t_1 \int_{\mathcal{C}} \mathrm{d}t_2\, G_{ik}(t,t_1)\,\Sigma_{kl}(t_1,t_2)\,G_{lj}(t_2,t')\,, \\
\Sigma_{ij}(t,t') &= \frac{i}{N}\,G_{ij}(t,t')\,\mathcal{D}_0(t,t') - x_i(t)\,\mathcal{D}_0(t,t')\,x_j(t')\,.
\end{aligned} \tag{79}$$

We see here that the equation for $\mathcal{G}$ is the expansion of the BVA equation in a series of $1/N$, truncated at first order.

Let us now specialize to the case of the quantum roll problem where $x_i(t) = 0$. In that case the two point inverse propagator for the x field is

$$\begin{aligned}
\mathcal{G}^{-1}_{ij}[\chi](t_1,t_2) &= \frac{\delta^2\Gamma_{\text{Large-N}}[x,\chi]}{\delta x_i(t_1)\,\delta x_j(t_2)} = G^{-1}_{ij}[\chi](t_1,t_2) + \Sigma_{ij}[\chi](t_1,t_2)\,, \\
\text{with} \qquad \Sigma_{ij}[\chi](t,t') &= \frac{i}{N}\,G_{ij}(t,t')\,\mathcal{D}_0(t,t')
\end{aligned} \tag{80}$$

However it is $\mathcal{G}^{(2)}_{ij}(t,t')$ which enters into Eq. (78) and not $\mathcal{G}_{ij}(t,t')$. Thus the solution for $\mathcal{G}_{ij}(t,t')$, which we might interpret as $\langle x_i(t)x_j(t')\rangle$, does not enter into the dynamics of the solution! *This* $\mathcal{G}_{ii}(t,t)$ is positive definite, but quickly blows up.

The vertex function $\Gamma_{ij}(t_1,t_2,t_3)$ is given by:

$$\begin{aligned}
\Gamma_{ij}(t_1,t_2,t_3) &= \frac{\delta\mathcal{G}^{-1}_{ij}[\chi](t_1,t_2)}{\delta\chi(t_3)} \\
&= \delta_{\mathcal{C}}(t_1,t_2)\delta_{\mathcal{C}}(t_2,t_3)\delta_{ij} - \frac{i}{N}\,G_{ij}(t_1,t_3)\,G_{ji}(t_3,t_2)\,\mathcal{D}_0(t_2,t_1) \\
&\quad - \frac{i}{N}\int_{\mathcal{C}}\mathrm{d}t_4\int_{\mathcal{C}}\mathrm{d}t_5\,G_{ij}(t_1,t_2)\,\mathcal{D}_0(t_1,t_4)\Lambda_0(t_4,t_5,t_3)\,\mathcal{D}_0(t_5,t_2)\,,
\end{aligned} \tag{81}$$

where the lowest order in $1/N$ 3-χ vertex is given by

$$\Lambda_0(t_4,t_5,t_3) = \delta\mathcal{D}_0^{-1}(t_4,t_5)\delta\chi(t_3) = -\frac{i}{N}\sum_{ijk} G_{ij}(t_4,t_3)\,G_{kl}(t_3,t_5)\,G_{li}(t_5,t_4)\,. \tag{82}$$

We immediately see that this is not an integral equation but again, is the lowest order in $1/N$ contribution to Eq. (63).

The inverse χ propagator gets $1/N$ corrections which are of two types, one is a self energy correction to the x propagator and the other is a new three loop graph containing two lowest order χ propagators. We find:

$$\mathcal{D}^{-1}(1,2) = \frac{\delta^2\Gamma_{\text{Large-N}}[x,\chi]}{\delta\chi(t_1)\,\delta\chi(t_2)}$$
$$= -\frac{1}{g}\delta_{\mathcal{C}}(1,2) - \Pi_0(1,2) - \sum_{ijkl}\int_{\mathcal{C}} \mathrm{d}t_3 \int_{\mathcal{C}} \mathrm{d}t_4\, G_{ij}(t_1,t_3)\,\Sigma_{jk}(t_3,t_4)\,G_{kl}(t_4,t_2)\,G_{li}(t_2,t_1)$$
$$+ \int_{\mathcal{C}} \mathrm{d}t_3 \int_{\mathcal{C}} \mathrm{d}t_4 \int_{\mathcal{C}} \mathrm{d}t_5 \int_{\mathcal{C}} \mathrm{d}t_6\, \Lambda_0(t_4,t_1,t_3)\,\mathcal{D}_0(t_3,t_5)\,\Lambda_0(t_5,t_2,t_6)\,\mathcal{D}_0(t_6,t_4)\,. \quad (83)$$

The last term in this equation is a $1/N$ correction to the vertex function. However, it is $\mathcal{D}_0$ and not $\mathcal{D}$ which enters Eq. (79), so that the BVA and the $1/N$ expansion will differ only by terms of order $1/N^2$. The BVA approximation treats x and χ on exactly the same footing, whereas the large-N expansion treats x exactly, but then expands in loops of χ. So at order $1/N^2$, the large-N approximation will contain graphs omitted from the BVA approximation, and vice-versa.

8 Results

In this section we present the results of exact numerical simulations of the quantum roll, using initial conditions described in our previous paper on the large-N approximation [8]. We choose as our dimensionful mass scale the second derivative of $V(r)$ at the minimum of the effective one dimensional potential $U(r)$. This mass scale was chosen to have value 2. In terms of this mass scale, the coupling constant as well as r_0 are of order one for all N. The exact manner in which g and r_0 runs with N is described in ref. [8].

In Figs. 4 through 6, we show the results for $\langle x^2(t)\rangle$ as a function of t, comparing the bare vertex, the dynamic Debye screening, and the large-N approximations to the exact solution, for $N = 3$, 4, 10, and 21. In Figs. 7 to 8, we show the same results for $\langle\chi(t)\rangle$ as a function of t, and in Figs. 9 through 11, we give the results for $\langle\chi^2(t)\rangle$.

In our previous studies of the large-N approximation[8], we found that the next to leading order large-N approximation had the feature that the effective potential was not defined at small x for $N \leq 20$, and it was not until N was greater than about 20 that the large-N expansion produced bounded values for $\langle x^2(t)\rangle$. This result is reproduced here. For the limit $N \to \infty$ the quantity $\langle x^2(t)\rangle$ corresponds to harmonic oscillations. At finite N, however, the exact solution for $N \geq 21$ has the property that the envelope of these oscillations contracts. As noted in the figures, only the bare vertex approximation attempts to follow this contraction. It succeeds up to a $t \approx 130$ before overshooting and completely damping out. This damping out is because it ignores quantum phase information present in the exact solution. In contrast to the next to leading order in large-N expansion, both the bare vertex and the dynamic Debye screening approximations have the feature that $\langle x^2(t)\rangle$

remains positive definite, as well as being bounded at all N. The dynamic Debye screening approximation works much better than the second order large-N approximation for N less that 20, but for N greater than 20, the reverse becomes true. However, neither approximation captures the true nonlinear shrinking of the envelope of the oscillations, even for N greater than 20.

Energy is conserved for the bare vertex and the second order large-N approximations, but not for the dynamic Debye screening approximations, as pointed out in section 6. This is a serious drawback to the dynamic Debye screening approximation.

In all these figures, one can see that the bare vertex approximation tries to follow the envelope of the exact curve, whereas the dynamic Debye screening approximation does not do so. This is particularly striking for the cases when N is less than 21, where the dynamic Debye screening approximation yield unphysically large values for the expectation values.

In the BVA approximation we observe that $\langle x^2(t) \rangle$ approches a constant value. It turns out that all the contributions to the energy in the BVA have the same feature that they asymptote to a fixed point. In Fig. 12 we show all four contributions to the energy at $N = 10$ to demonstrate this fact. In contrast, as seen in the very long time run shown in Fig. 11, the exact solutions exhibit "recurrence" patterns of motion which are not captured in the BVA. The expectation values of the components contributing to the energy remain positive in the the bare vertex and dynamic Debye screening approximations. In contrast, they often go negative in the large-N approximation.

In summary we have found that both resummation methods described here, the BVA and the DDSA, produce positive definite and apparently bounded results for expectation values. The bare vertex approximation appears to provide the best description of the motion, but cannot describe recurrences of the motion. Still, it provides an energy conserving and reasonably accurate description of the motion, and is a great improvement over the next to leading order large-N approximation.

Acknowledgements

We wish to thank Salman Habib for helpful discussions on understanding the numerical simulations. We wish to thank Prof. Gabor Kalman for explaining relevant plasma conductivity approximations, and Emil Mottola for suggesting our study of the "dynamic Debye screening" approximation and explaining its derivation from the CJT formalism. JFD is supported in part by the U.S. Department of Energy under grant DE-FG02-88ER40410. He would like to thank the T-8 theory group at LANL, and the Institute for Nuclear Theory at the University of Washington, for hospitatility during the course of this work.

References

[1] A. H. Guth and S.-Y. Pi, Phys. Rev. D **32**, 1899 (1985).

[2] F. Cooper, S.-Y. Pi and P. Stancioff, Phys. Rev. D **34**, 3831 (1986).

[3] G. J. Cheetham and E. J. Copeland, Phys. Rev. D **53** R4125 (1996).

[4] Robert Kraichnan, J. Math. Phys. **2**, 124 (1961).

[5] D. K. Hong, V. A. Miransky, I. A. Shovkovy, and L. C. R. Wijewardhana, Phys. Rev. D **61**, 056001, (2000) [http://arXiv.org/abs/hep-th/9905116].

[6] F. Cooper, S. Habib, Y. Kluger, E. Mottola, J. P. Paz, and P. R. Anderson, Phys. Rev. D **50**, 2848 (1994) [http://arXiv.org/abs/hep-ph/9405352];
F. Cooper, Y. Kluger, E. Mottola and J. P. Paz, Phys. Rev. D **51**, 2377 (1995);
Y. Kluger, F. Cooper, E. Mottola, J. P. Paz, A. Kovner, Nucl. Phys. A590, 581c (1995);
M. A. Lampert, J. F. Dawson and F. Cooper, Phys. Rev. D **54**, 2213 (1996);
F. Cooper, Y. Kluger, and E. Mottola, Phys. Rev. C **54**, 3298 (1996).

[7] A. K. Kerman and S. E. Koonin, Ann. Phys. 100, 332 (1976);
R. Jackiw and A. K. Kerman, Phys. Lett. A **71**, 158 (1979);
F. Cooper, S.-Y. Pi and P. Stancioff, Phys. Rev. D **34**, 3831 (1986);
F. Cooper and E. Mottola, Phys. Rev. D **36**, 3114 (1987);
S.-Y. Pi and M. Samiullah, Phys. Rev. D **36**, 3128 (1987);
D. Boyanovsky and H. J. de Vega, Phys. Rev. D **47**, 2343 (1993);
D. Boyanovsky, H. J. de Vega, R. Holman, D. S. Lee, and A. Singh, Phys. Rev. D **51**, 4419 (1995);
D. Vautherin and T. Matsui, Phys. Rev. D **55**, 4492, (1997).

[8] B. Mihaila, J. F. Dawson, F. Cooper, S. Habib, and T. Athan, *Dynamics of the quantum mechanical $O(N)$ model*, (Submitted to Phys. Rev. D) [http://arXiv.org/abs/hep-ph/0003105].

[9] C. Oberman, A. Ron, and J. Dawson, Phys. Fluids **5**, 1514 (1962).

[10] M. G. Kivelson and D. F. Dubois, Phys. Fluids **7**, 1578 (1964).

[11] J.-P. Blaizot and G. Ripka, *Quantum Theory of Finite Systems*, (MIT press, Cambridge, MA; 1986), p. 156.

[12] J. Schwinger, J. Math. Phys. **2**, 407 (1961);
P. M. Bakshi and K. T. Mahanthappa, J. Math. Phys. **4**, 1 (1963); **4**, 12 (1963);
L. V. Keldysh, Zh. Eksp. Teo. Fiz. **47**, 1515 (1964) [Sov. Phys. JETP **20**, 1018 (1965)];
G. Zhou, Z. Su, B. Hao and L. Yu, Phys. Rep. **118**, 1 (1985);
F. Cooper, J. F. Dawson, S. Habib, Y. Kluger, D. Meredith and H. Shepard, Physica D **83**, 74 (1995).

[13] C. Itzykson and J-B. Zuber, *Quantum Field Theory*, (McGraw-Hill, 1980), p. 476.

[14] F. Cooper, G. Guralnik, R. W. Haymaker, K. Tamvakis,
Phys. Rev. D **20**, 3336 (1979).

[15] M. M. Cornwall, R. Jackiw, and E. Tomboulis,
Phys. Rev. D **10**, 2428 (1974).

[16] C. De Dominicis, J. Math. Phys. **3**, 983 (1962);
C. De Dominicis and P. C. Martin,
J. Math. Phys. **5**, 14 (1964), *ibid*, **5**, 31 (1964).

[17] H. D. Dahmen and G. Jona-Lasinio,
Nuovo Cim., **52A**, 807 (1967); *ibid*, **62A**, 889 (1969).

[18] A. N. Vasil'ev and A. K. Kazanskii,
Teor. Mat. Fiz., **12**, 352 (1972); *ibid*, **14**, 289 (1973).

[19] Emil Mottola (private communication).

[20] B. Mihaila, J. F. Dawson, and F. Cooper,
Phys. Rev. D **56**, 5400 (1997) [http://arXiv.org/abs/hep-ph/9705354].

[21] B. Mihaila and I. Mihaila, http://arXiv.org/abs/physics/9901005.

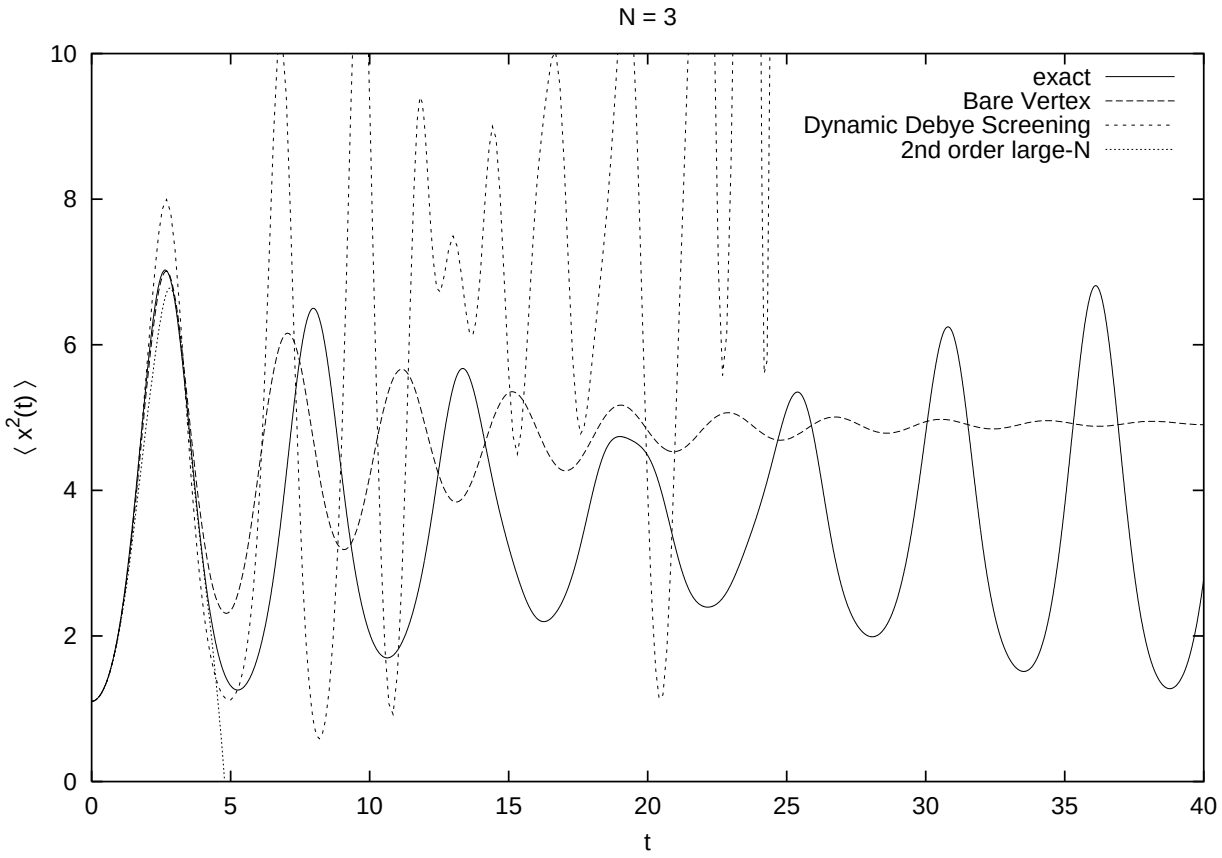

Figure 4: Plot of $\langle x^2(t) \rangle$ as a function of t, comparing the bare vertex, the dynamic Debye screening, and the large-N approximations to the exact solution, for $N = 3$.

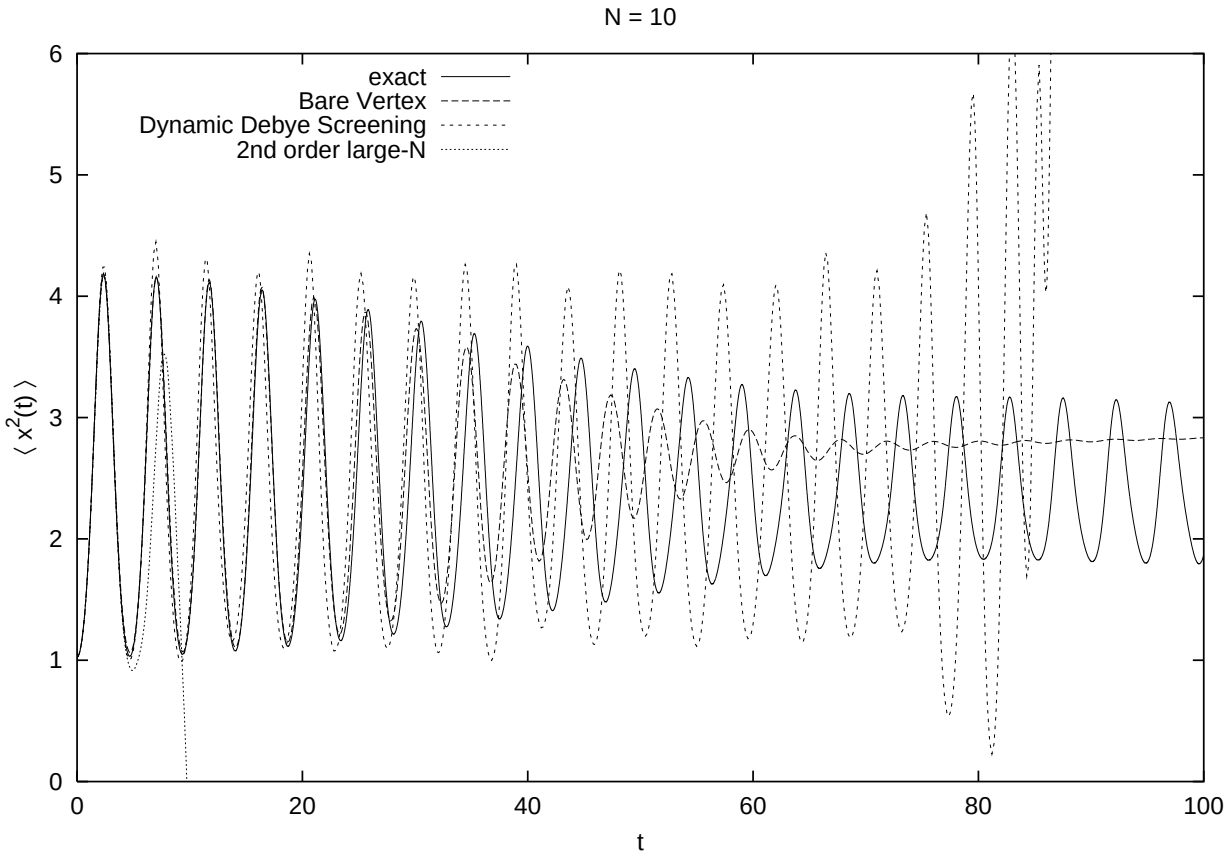

Figure 5: Plot of $\langle x^2(t) \rangle$ as a function of t, comparing the bare vertex, the dynamic Debye screening, and the large-N approximations to the exact solution, for $N = 10$.

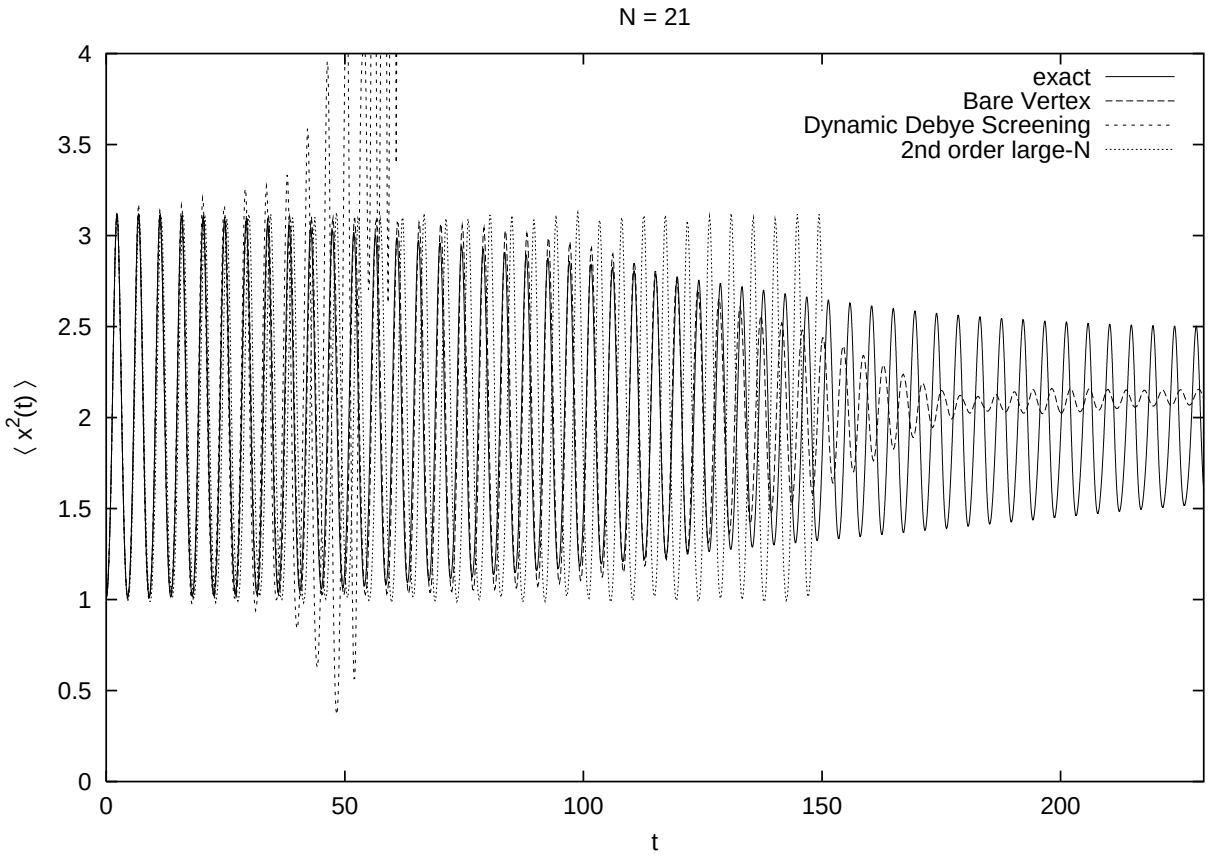

Figure 6: Plot of $\langle x^2(t) \rangle$ as a function of t, comparing the bare vertex, the dynamic Debye screening, and the large-N approximations to the exact solution, for $N = 21$.

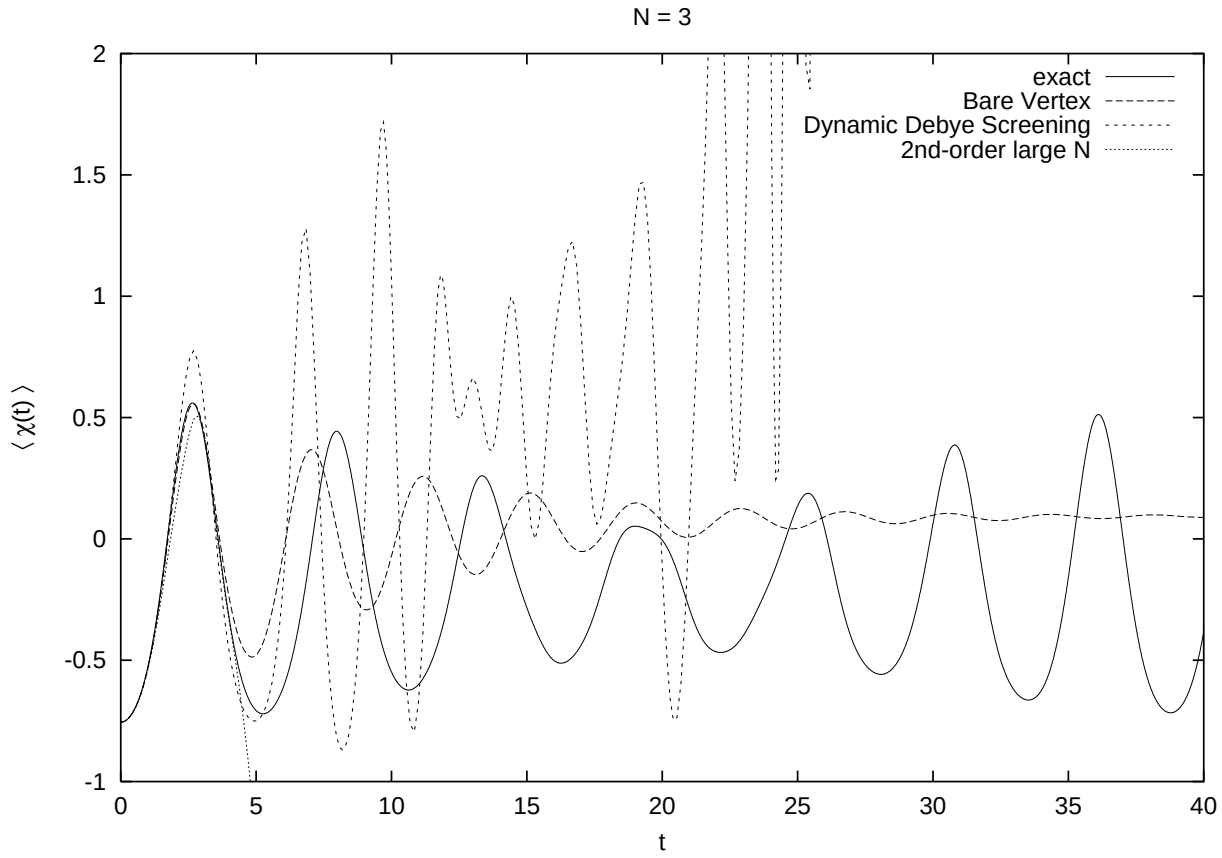

Figure 7: Plot of $\langle \chi(t) \rangle$ as a function of t, comparing the bare vertex, the dynamic Debye screening, and the large-N approximations to the exact solution, for $N = 3$.

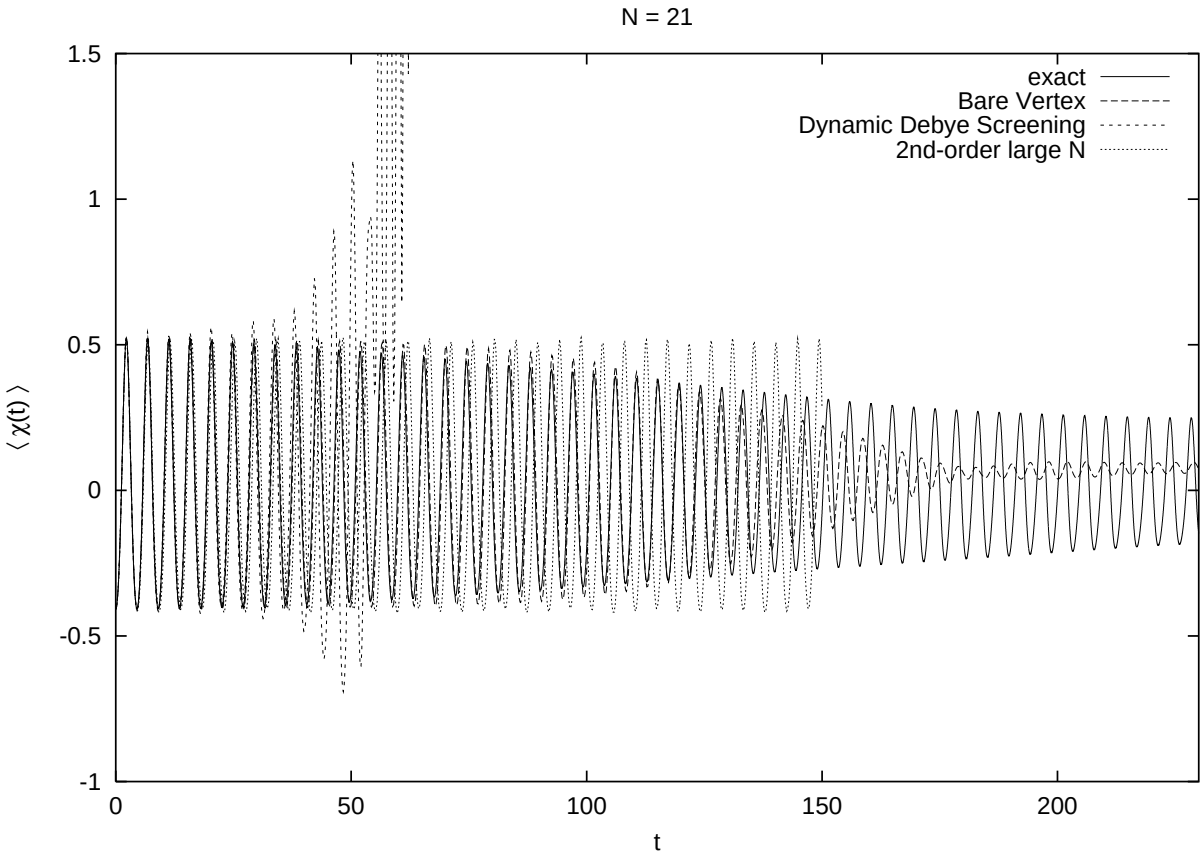

Figure 8: Plot of $\langle \chi(t) \rangle$ as a function of t, comparing the bare vertex, the dynamic Debye screening, and the large-N approximations to the exact solution, for $N = 21$.

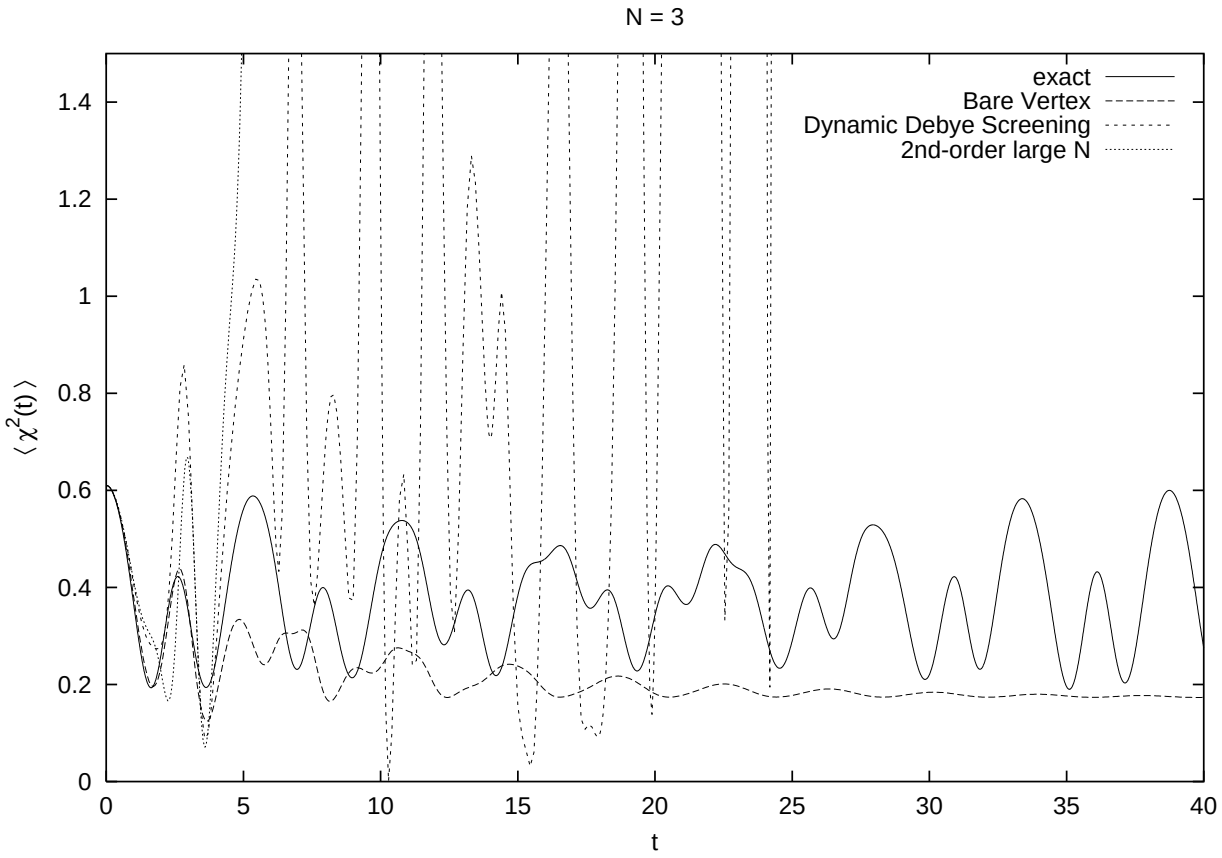

Figure 9: Plot of $\langle \chi^2(t) \rangle$ as a function of t, comparing the bare vertex, the dynamic Debye screening, and the large-N approximations to the exact solution for $N = 3$.

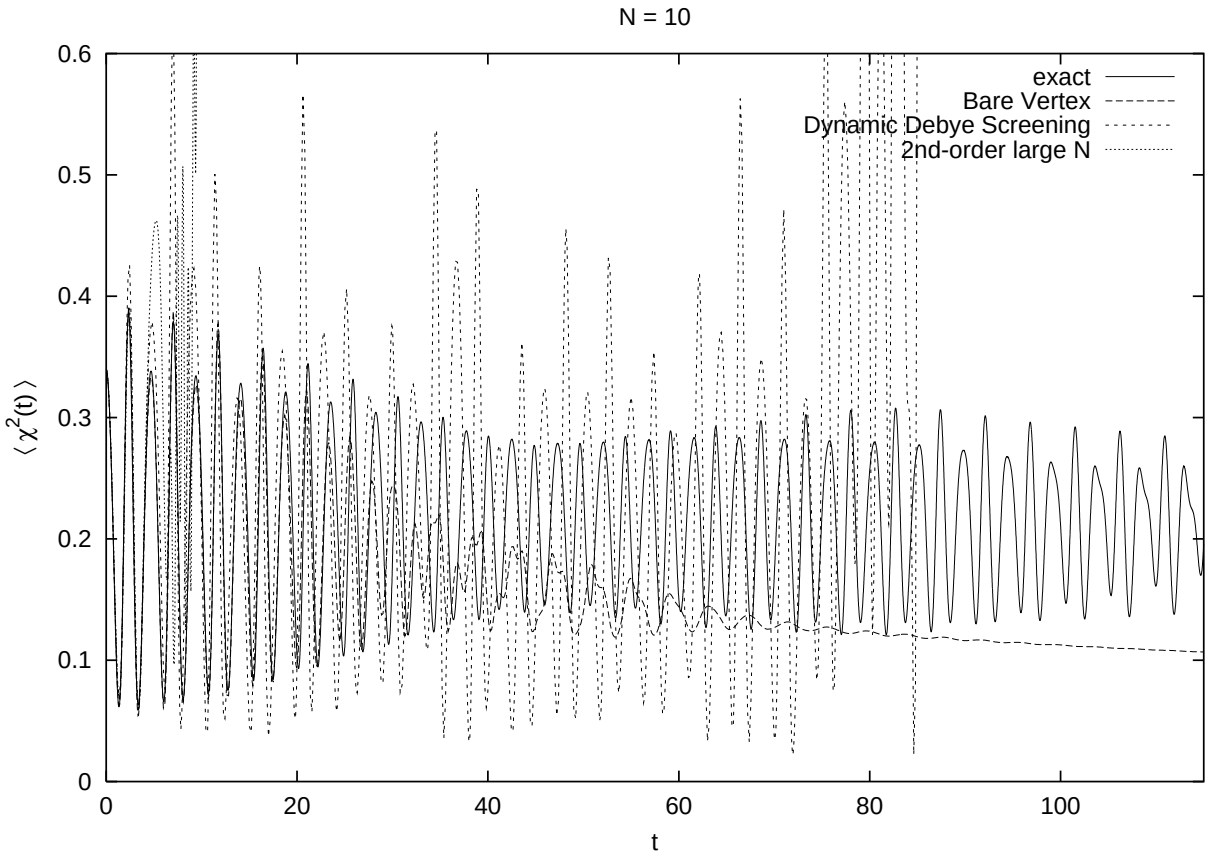

Figure 10: Plot of $\langle \chi^2(t) \rangle$ as a function of t, comparing the bare vertex, the dynamic Debye screening, and the large-N approximations to the exact solution for $N = 10$.

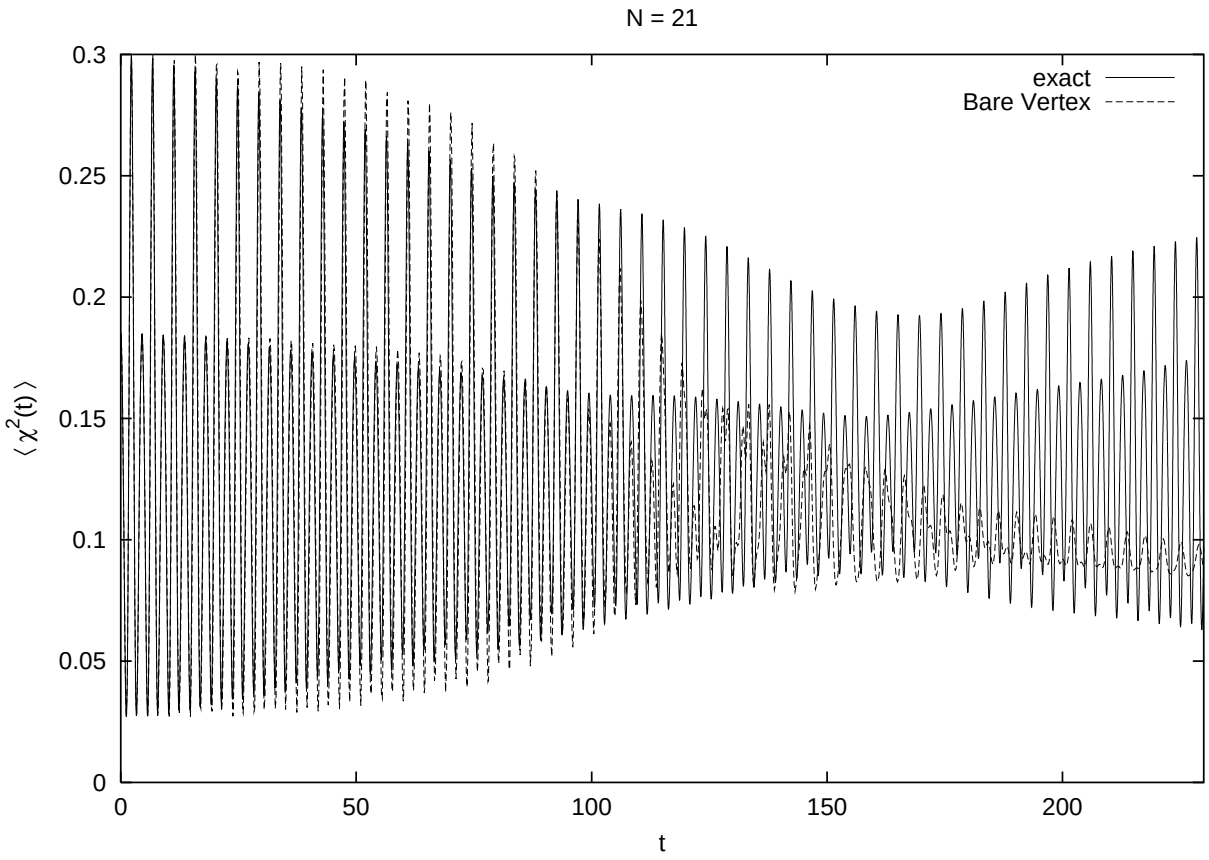

Figure 11: Plot of $\langle \chi^2(t) \rangle$ as a function of t, comparing the bare vertex approximation to the exact solution for $N = 21$.

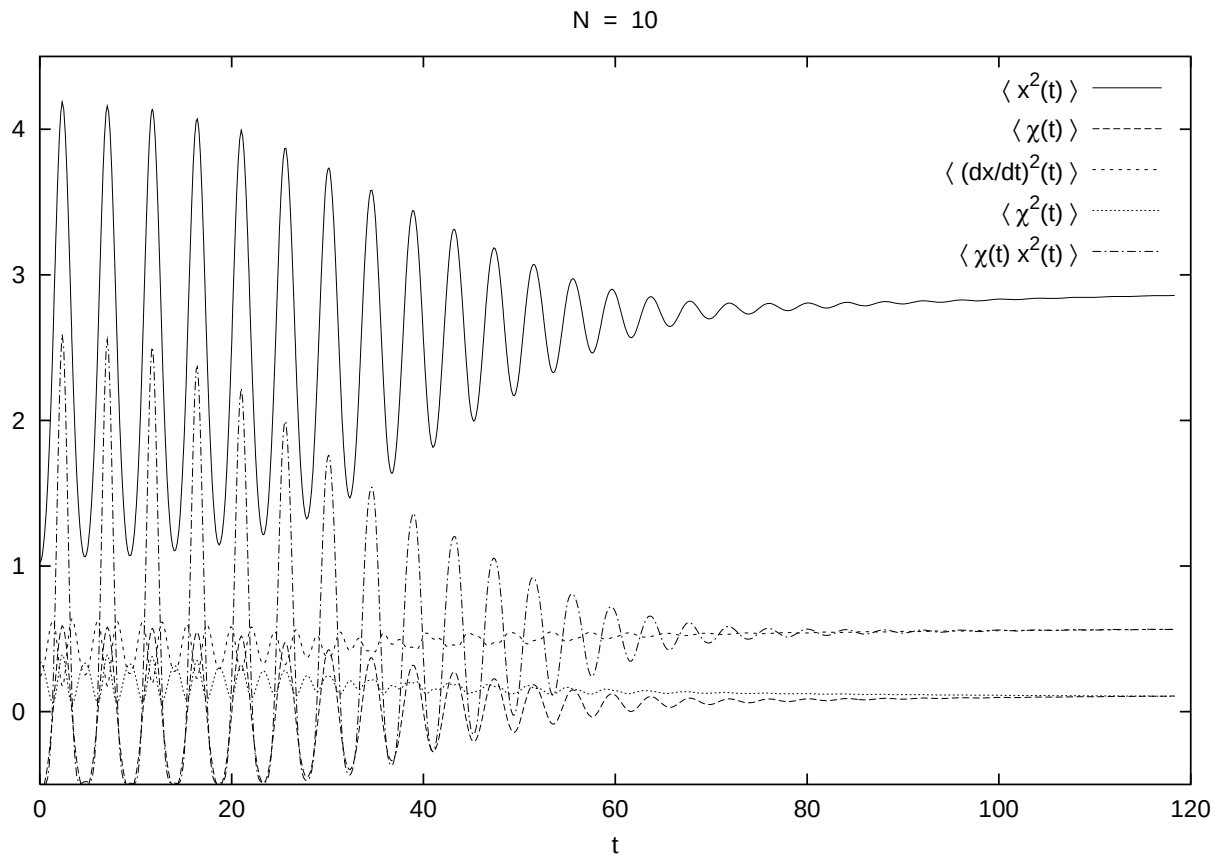

Figure 12: Plot of various contributions to the energy for the bare vertex approximation as a function of t for $N = 10$.